Measurement of attosecond XUV pulses generated with polarization gating by two-dimensional photoelectron spectroscopy

Shambhu Ghimire*, Ximao Feng and Zenghu Chang
J. R. Macdonald Laboratory, Kansas State University, Manhattan, KS 66506

ABSTRACT

We report on our high speed camera designed for temporal characterization of attosecond pulses (1as =10^{-18}s) generated with the polarization gating technique. The uniform external magnetic field applied on the time-of-flight spectrometer enlarges the acceptance angle (up to 65^o for ~20-eV photoelectrons). By collecting two-dimensional momentum images of the photoelectrons, which are ejected by the XUV pulses and streaked directly by the co-propagating polarization gating electric field, we expect to derive the information about the XUV pulses. After the characterization of XUV pulses, the same setup can be used to study complex dynamics of electrons in atoms and molecules with time-resolved spectroscopy.

Keywords: Attosecond Pulses, Ultrafast measurements, Photoionization, Polarization Gating

1. INTRODUCTION

Time-resolved measurements with attosecond pulses enable us to study the dynamic behavior of electrons in atoms and molecules. Higher-order harmonic generation (HHG) using few-cycle laser pulses has become a well established method for producing attosecond pulses in the last several years [1, 2]. The temporal characterization of such pulses has, however, become a challenge as the conventional techniques for characterizing light pulses, such as FROG [3], cannot be easily adopted at the XUV region mainly due to the lack of a suitable non-linear medium at the available intensities. As an alternative, a so-called Attosecond Streak Camera had been proposed [4] and realized in practice for characterizing attosecond pulses [2, 5]. In these experiments, the XUV pulses were used to photo-ionize a second target gas in the presence of a linearly polarized intense optical field. By measuring the energy or momentum change (streak) on the photoelectrons by the laser field, the pulse duration of the XUV pulse was measured. Most of these high speed cameras reported so far were however limited to one-dimensional photoelectron energy measurement and had an acceptance angle of only a few degrees. Here, we report on our design of such a high speed camera which is capable of measuring electron momenta in two dimensions with a much larger acceptance angle. We generated the XUV pulses by the polarization gating technique taking advantage of the fact that the HHG process is highly sensitive to the polarization of the driving laser field [6]. One different feature of our design of the measurement from Ref. [2] is that we use the polarization gating field directly to streak the photoelectrons instead of introducing a second laser beam as the pumping source. With this method the streaking beam can always be inside the same vacuum chamber as the XUV beam and thus make the experimental setup simpler and less sensitive to possible interferometric vibrations.

2. PRINCIPLE OF CHARACTERIZING ATTOSECOND XUV PULSES

2.1 Angular distribution of photoelectrons

Since in our experiment, we intended to collect photoelectrons in a large acceptance angle, we needed to take the angular distribution of photoelectrons into consideration. In the dipole approximation, the angular distribution of the emitted atomic photoelectrons can be written as [7]:

$$\frac{d\sigma}{d\Omega}(\theta) = \frac{\sigma}{4\pi}\left[1 + \frac{\beta}{2}\left(3\cos^2\theta - 1\right)\right] \quad (1)$$

*Current address of the author is Department of physics, University of Michigan, Ann Arbor, MI, 48109

*For further information please contact shambhu@umich.edu or chang@phys.ksu.edu

Ultrafast X-Ray Sources and Detectors, edited by Zenghu Chang, George A. Kyrala, Jean-Claude Kieffer,
Proc. of SPIE Vol. 6703, 67030F, (2007) · 0277-786X/07/$18 · doi: 10.1117/12.737580

where σ is the total cross section, Ω is the solid angle, β is the angular distribution parameter, and θ is the angle between the direction of the electron emission and the electric field vector of the polarized laser beam.

In this report, the photoelectrons were produced from the 2*p* orbital of Ne atoms. The total cross section was set to be 8Mb [8] (1 Mb = 10^{-18} cm^{-2}) and the angular distribution parameter values were given in Ref. [9].

2.2 Streaking with ellipticity varying strong laser field

The principle of polarization gating [10] is shown in Fig. 1. It starts with a linearly polarized electric field:

$$\vec{E}_L(t) = E_{0L}\left[e^{-2\ln(2)(t/\tau_L)^2}\right]\times\cos(\omega t)\hat{k} \tag{2}$$

where $\vec{E}_{0L}$ is the peak field amplitude, τ_L is the pulse duration, and ω is the angular frequency. For simplicity, we have set the phase to be equal to zero. We are taking a coordinate frame such that the incoming beam propagation direction is $\hat{j}$, the electric field vector direction is horizontal along $\hat{k}$, and the vertical direction is defined as $\hat{i}$. After passing through the multi-order quartz wave plate, whose optical axis is 45 degrees relative to the incoming beam electric field, the original pulse is divided into two linear components (o-ray and e-ray) with a time delay T_d between them. The following quarter wave plate turns the two components into two circularly polarized pulses, each of which is formed by two linear pulses perpendicular to each other and with a time delay of *T*/4 between them. *T* is the optical cycle and equal to 2.67 fs for our 800-nm-wavelength laser. The final polarization gating electric field can be expressed as:

$$\vec{E}_C(t) = (E_{0L}/2)\left[e^{-2\ln(2)((t+T_d/2+T/8)/\tau_L)^2} + e^{-2\ln(2)((t-T_d/2+T/8)/\tau_L)^2}\right]\cos(\omega t)\hat{k} +$$
$$(E_{0L}/2)\left[e^{-2\ln(2)((t+T_d/2-T/8)/\tau_L)^2} - e^{-2\ln(2)((t-T_d/2-T/8)/\tau_L)^2}\right]\sin(\omega t)\hat{i}\,. \tag{3}$$

The two components of the polarization gating electric field are plotted in Fig. 2. From the figure, we can see that there is only a small time interval near $t = 0$ where the ellipticity is small. Since HHG is inherently sensitive to the polarization of the driving electric field, attosecond pulses can only be produced within this short period of time (polarization gate). If the gate is small enough (< T/2), only a single recombination channel of the detached electron with its parent ion is possible, giving rise to a single attosecond pulse.

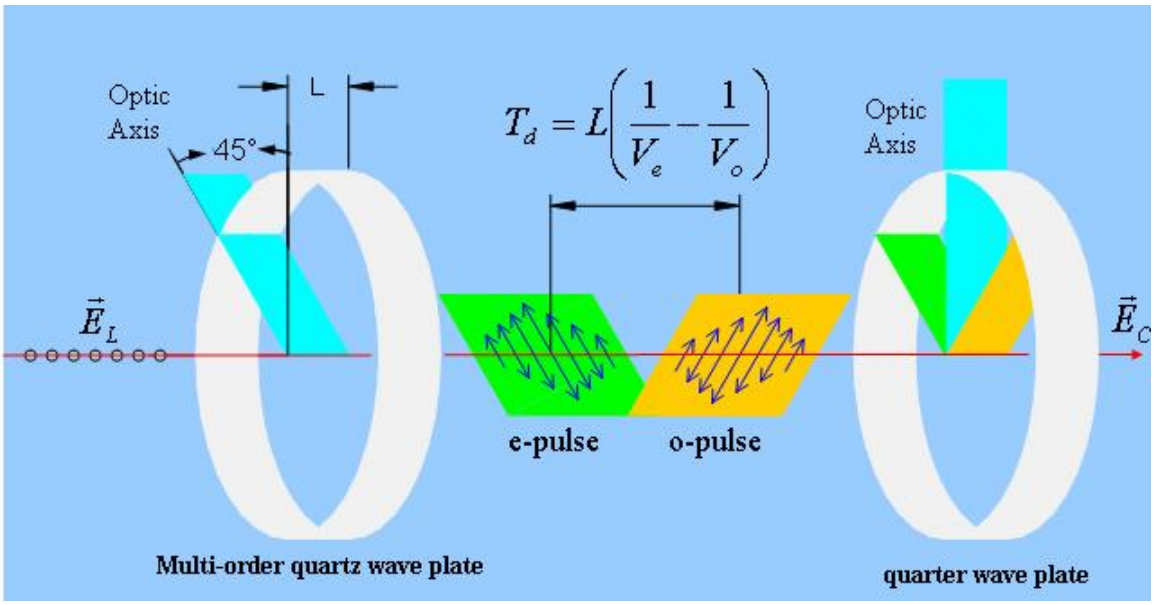

Figure 1. The principle of polarization gating. The optics includes a multi-order whole wave quartz wave plate and a zero-order achromatic quarter wave plate. The direction of the optic axis of the quartz plate is set 45° to the initial

direction of polarization of the laser, and that of the quarter wave plate is along the direction of polarization of the laser.

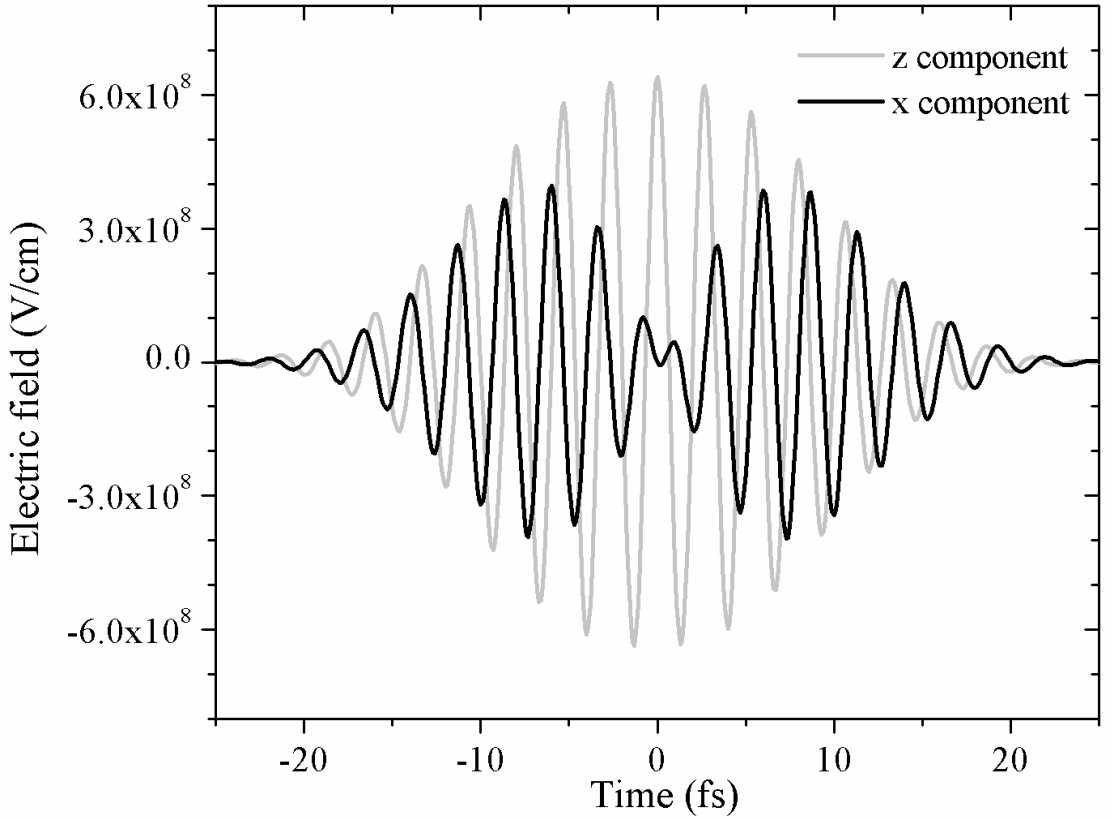

Figure 2. The two components of the electric fields of the ellipticity varying pulse. In the calculation, it is assumed that the laser pulse duration $\tau = 10$ fs, the time delay between the two circularly polarized pulses is $5T$ (T = 2.67 fs), and the initial linear polarized pulses have a peak intensity of 1.2×10^{15} W/cm^2.

The momentum change of the photoelectrons provided with the above electric field is:

$$\Delta\vec{p} = -e\int_{t_b}^{\infty} \vec{E}_C(t')dt' \tag{4}$$

In Eq. (4), t_b represents the birth time of the electron. We have calculated the laser assisted two-dimensional momentum spectra for different delays, as shown in Fig 3. In this calculation we have assumed that the duration of XUV pulses is 100 as.

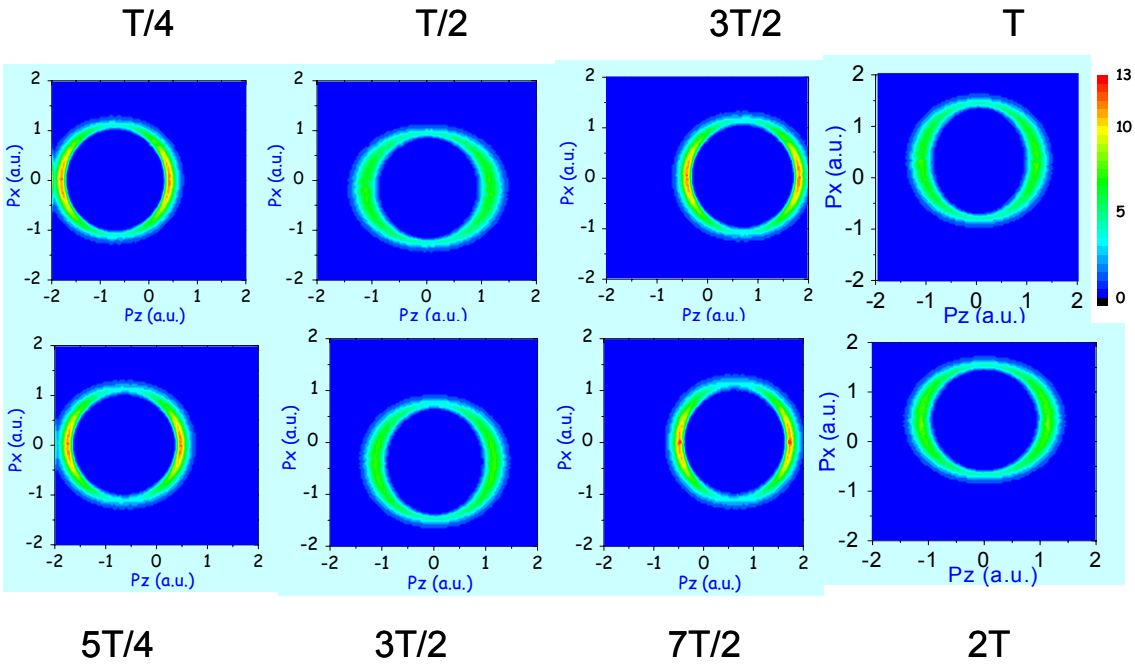

Figure 3. Calculated two-dimensional momentum maps of the photoelectrons produced by single attosecond pulses and streaked in an ellipticity varying strong laser field. The label at the top or bottom of each graph represents the time when the electron is born.

3. EXPERIMENTAL SETUP

The experimental setup of our design of the attosecond streak camera is shown in Fig.4. It mainly consisted of four sections: (i) hollow-core fiber and chirped mirrors; (ii) HHG using polarization gating; (iii) pump-probe; and (iv) time-of-flight spectrometer for measuring momentum of photoelectrons.

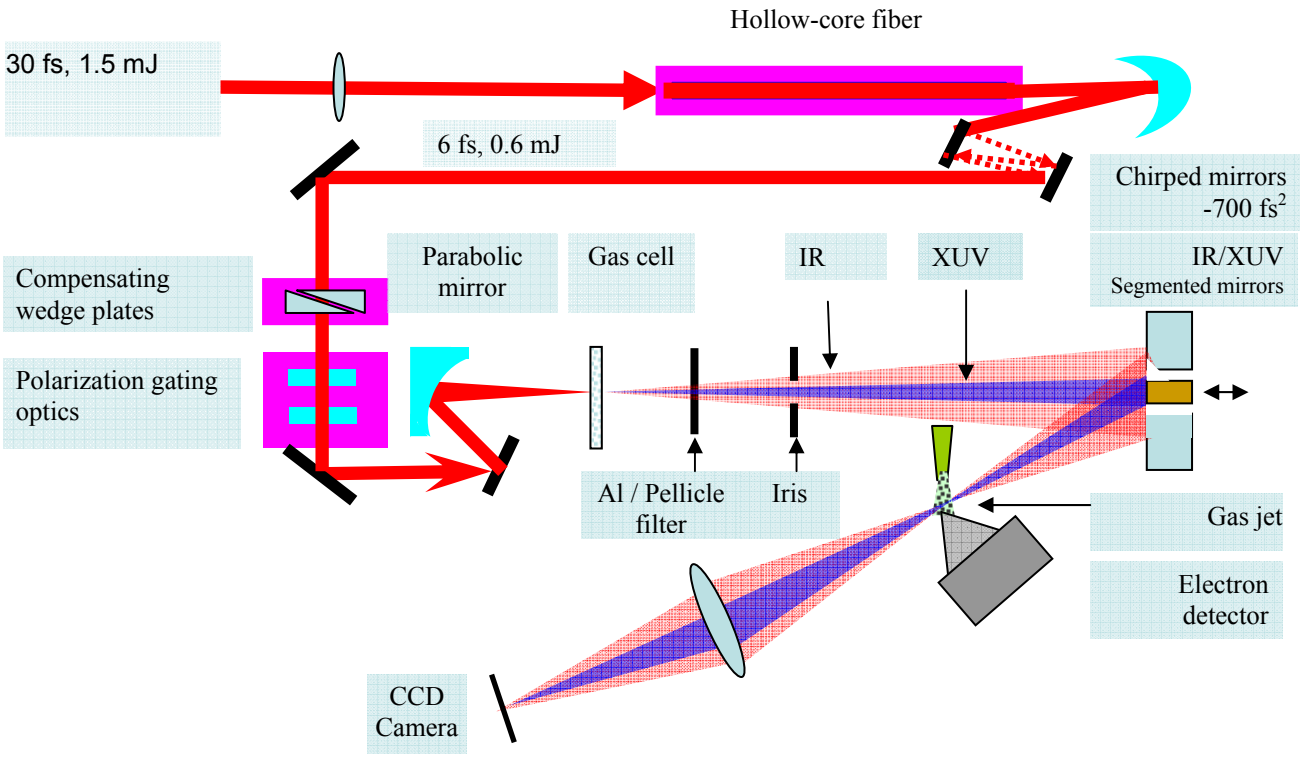

Figure 4. A schematic of the experimental setup for producing and measuring attosecond pulses. Laser pulses of 30 fs in duration and about 1.5-mJ energy were coupled into a hollow-core fiber filled with Ne gas and compressed with the chirped mirrors up to 6fs at pulse energy of 0.6mJ. After passing through the polarization gating optics the beam was focused with a parabolic mirror into an Ar gas cell. Following HHG, the XUV and IR beams were separated with a spatial filter and focused on a Ne gas target. The emitted photoelectrons were guided by an external magnetic field to the time-of-flight spectrometer. An imaging system was developed, which is simplified in this picture, for monitoring the overlap of the two laser foci formed by the segmented mirrors assembly when the laser was shining on both of the mirrors.

The experiment was carried out at the Kansas Light Source (KLS) of Kansas State University. KLS is a laser system delivering laser pulses of 30 fs in duration, 3 mJ of energy centered around 800 nm with a repetition rate of 1 kHz. For this experiment, a fraction of the beam was focused into the hollow-core fiber, filled with Ne gas at a pressure of 2.4 bars for spectral broadening. The pulse was then compressed in time using a set of chirped mirrors. The compensating wedge plates were introduced in the beam line in order to fine tune the dispersion. This linearly polarized beam was converted to an ellipticity varying pulse using polarization gating optics which consists of a quartz plate and a quarter wave plate. The laser polarization was set horizontal before entering the hollow fiber. The quartz plate was placed with its optic axis at 45 degrees with respect to the laser polarization (horizontal), and the optic axis of the quarter wave plate was set at the same direction as the laser polarization. Then, the beam was focused by a parabolic mirror with a focal length of 30 cm into an Ar gas cell of 1.4 mm inner diameter. Two small holes were drilled by the laser on the gas cell at the entrance and exit. These two holes served for creating differential pressure between the gas jet and the HHG chamber. The gas pressure and the jet position relative to the focus spot were optimized by observing the radial intensity of the beam on the removable MCP and phosphor screen on the downstream of the beam line.

Following HHG, the XUV and the residual IR co-propagate in the vacuum chamber. In order to use these two beams for the pump-probe application it was required to spatially separate them and introduce a delay stage between them. We used a spatial filter on the downstream of the HHG section for their spatial separation which consisted of an aluminum foil of 200 nm in thickness at the center for transmitting only XUV and a 7.5-μm-thickness annular Kapton pellicle outside for transmitting only laser. The IR beam intensity was controlled with an iris mounted after the filter. At the end of the setup, at 97.5cm from the position of the first laser focus, there was a two-component focusing mirror assembly. The central mirror was a broadband reflective Mo-Si mirror of diameter 12.5mm for focusing the XUV beam. The outer annular mirror was of outer diameter 50.8 mm and coated with silver for focusing the IR beam. The two mirrors were aligned on the same spherical plane and both had a focal length of 30 cm.

A 120-mm-diameter time and position sensitive detector (MCP and delay line anode, RoentDek) was used to detect the positions and measure the energies and momenta of the photoelectrons. The detector was set perpendicular to the direction of laser polarization at 15 cm from the interaction region. A cone with a 3-mm hole separated the detector chamber and the interaction chamber by creating a pressure difference of two orders of magnitude. We used a metal tube of inner diameter 100 μm as a gas jet. In order to increase the acceptance angle for the photoelectrons, we used an approximately uniform external magnetic field (~3.5Gauss) which was applied by two coils on both sides of the setup.

In order to test this setup, we used linearly polarized laser pulses of duration ~30 fs to generate a train of attosecond pulses (discrete harmonic spectrum in spectral domain) from Ar gas. One momentum image of the measured corresponding photoelectrons is shown in Fig. 5. From right to left, the discrete lines are formed by photoelectrons produced by 23rd, 25th, 27th and 31st harmonics, respectively. In this particular measurement the acceptance angle for the 25th harmonics was found to be 65^{o}.

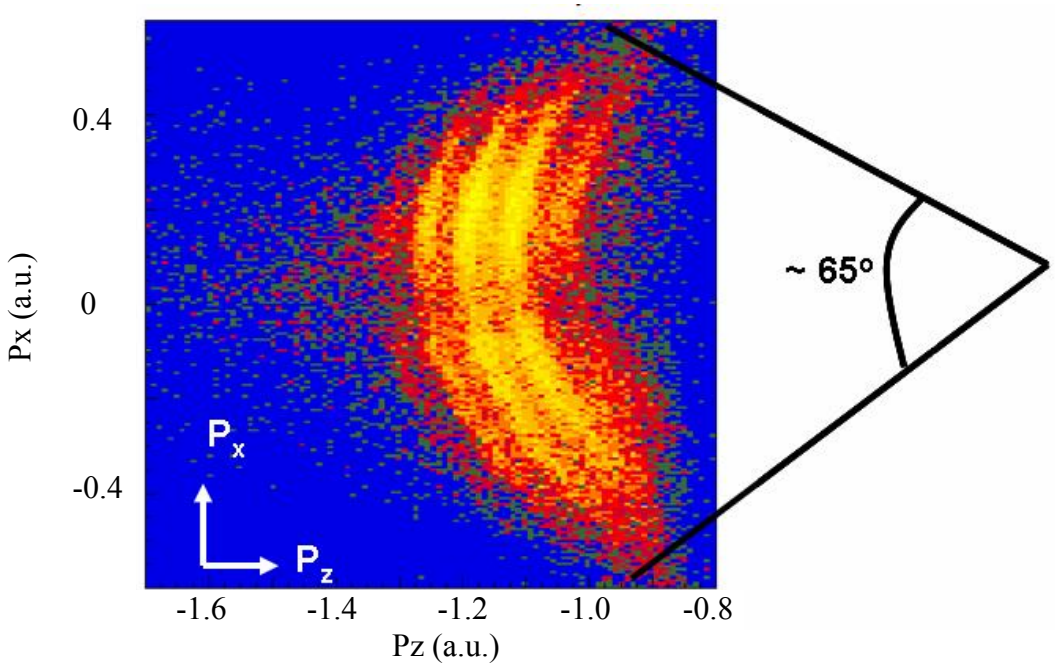

Figure 5. Measured two-dimensional momentum image of photoelectrons produced by different higher order harmonics. The acceptance angle for the photoelectrons produced by the 25th harmonic is shown on the right. Note that the high-harmonics were produced by linearly polarized laser pulses of duration ~30 fs. It was done in the same beam line described above but by evacuating the hollow-core fiber and setting the optic axis of all the birefringence optics along the initial direction of polarization of the laser.

4. LASER ASSISTED PHOTOELECTRON ENERGY/MOMENTUM SPECTRUM

The modification in the photoelectron spectrum in the presence of a strong laser field has been studied extensively in the past few years [11 - 13]. It is believed that this modification is due to the momentum transfer between the emitted photoelectrons and the strong laser field. As a result, when the duration of the XUV pulse is longer than the laser cycle, in addition to the main peaks, sidebands are produced on the laser assisted photoelectron spectrum. This effect has been understood as a free-free transition: the electron absorbs or emits one photon from or to the IR during the photoionization process and transfers from one free state to another. In addition, the total spectrum shifts towards lower energy due to an increase in the binding energy of the atoms in the presence of the laser. The energy of a sideband is given by the following [12]:

$$E_s = h\gamma_{xuv} \pm h\gamma_{IR} - I_P - U_p^{IR} \tag{5}$$

where $h\gamma_{xuv}$ is the energy of the XUV photons, $h\gamma_{IR}$ is the energy of the IR photons, I_p is the ionization potential of the interacting medium, and U_P^{IR} is the ponderomotive energy.

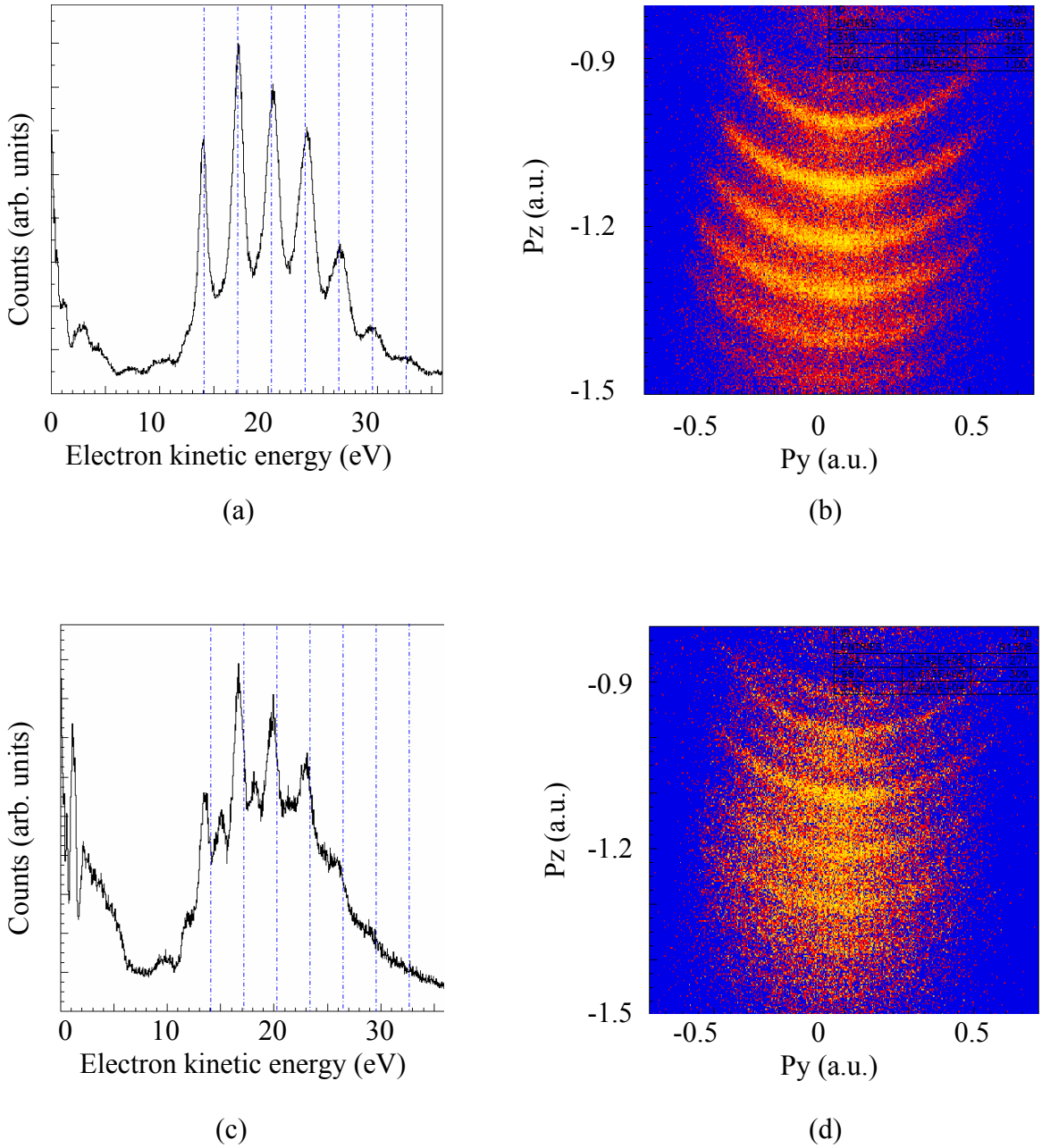

Figure 6. Measured energy (a) and momentum (b) spectra of photoelectrons without laser. Measured energy (c) and momentum (d) spectra of photoelectrons in the presence of a strong laser field. Again note that the high harmonics were produced by a linearly polarized laser pulse of duration ~30 fs. It was done in the same beam line described above but by evacuating the hollow-core fiber and setting the optic axis of all the birefringence optics along the initial direction of polarization of the laser.

The measured primary photoelectron energy and momentum spectra with long linearly polarized optical pulses are shown in Fig. 6 (a) and (b), respectively. The discrete structures correspond to the photoelectrons produced by different higher-order harmonics. Similarly, the laser assisted energy and momentum spectra are shown in Fig. 6 (c) and (d), respectively. One can notice that the spectra shifted towards the lower energy side by 0.5 eV due to the presence of the laser. The ponderomotive shift can be used to estimate the intensity of the laser with the following relation:

$$U_p^{IR}(eV) = 9.33 \times 10^{-14} I(W/cm^2)\lambda^2(\mu m) \quad (6)$$

This relation implies that our streaking laser intensity in this particular measurement was around 8.2×10^{12} W/cm^2.

5. CONCLUSION AND FUTURE PLAN

We have designed an attosecond streak camera setup with new features. In this setup, we can collect two-dimensional momentum images of photoelectrons in a large acceptance angle. The measured maximum acceptance angle was ~65^o for 20-eV photoelectrons. As a preliminary measurement, using linearly polarized laser pulses (~30fs), we have generated high harmonics and observed sidebands in their laser-assisted photoelectron spectra, which is an indicator that the overlap between the XUV and the IR beam is achieved. We anticipate that this setup can be used for real time characterization of single attosecond pulses produced with the polarization gating technique. After achieving this primary goal, this workstation can be used to explore the dynamics of the electrons in atoms and molecules on an attosecond timescale.

6. ACKNOWLEDGEMENT

This work was supported by the Department of Energy, Department of Defense (MURI), and National Science Foundation. The authors would like to thank Chris Nakamura, Sabih Khan and He Wang for their help in this experiment.

REFERENCES

1. E. Goulielmakis *et al*., Science, 305, 1267 (2004)
2. G. Sansone *et al.,* Science, 314, 443 (2006)
3. D. J. Kane and R. Trebino, IEEE J. Quantum Electron. 29, 571 (1993)
4. E. Constant *et al.*, Phys. Rev. A, 56, 3870-3878 (1997)
5. M. Drescher *et al*., Science, 291, 1923 (2001)
6. B. Shan, S. Ghimire and Z. Chang, J. of Mod. Opt., 52, 2-3, 277-283 (2005)
7. N. M. Kabachnik and I. P. Sazhina, J. Phys. B 17, 1335 (1984)
8. J. M. Bizau and F. Wuilleumier, J. Electron Spectrosc. Relat. Phenom. 71, 205 (1995)
9. F. Wuilleumier and M. O. Krause, J. Electron Spectrosc. Relat. Phenom. 15, 15 (1979)
10. Z. Chang, Phys. Rev. A, 70, 043803 (2004)
11. T. E. Golver *et al.,* Phys. Rev. Lett. 76, 2468 (1996)
12. P. M. Paul *et al*. Nature, 292, 1683 (2001)
13. M. Drescher *et al,* J. Phys. B, 38, S727 (2005)